

ARTICLES

An RNA-dependent RNA polymerase formed by TERT and the *RMRP* RNA

Yoshiko Maida¹, Mami Yasukawa¹, Miho Furuuchi¹, Timo Lassmann², Richard Possemato³, Naoko Okamoto¹, Vivi Kasim¹, Yoshihide Hayashizaki², William C. Hahn^{3,4} & Kenkichi Masutomi^{1,5}

Constitutive expression of telomerase in human cells prevents the onset of senescence and crisis by maintaining telomere homeostasis. However, accumulating evidence suggests that the human telomerase reverse transcriptase catalytic subunit (TERT) contributes to cell physiology independently of its ability to elongate telomeres. Here we show that TERT interacts with the RNA component of mitochondrial RNA processing endoribonuclease (*RMRP*), a gene that is mutated in the inherited pleiotropic syndrome cartilage–hair hypoplasia. Human TERT and *RMRP* form a distinct ribonucleoprotein complex that has RNA-dependent RNA polymerase (RdRP) activity and produces double-stranded RNAs that can be processed into small interfering RNA in a Dicer (also known as *DICER1*)-dependent manner. These observations identify a mammalian RdRP composed of TERT in complex with *RMRP*.

Telomerase is a ribonucleoprotein complex that elongates telomeres. Although several proteins interact with telomerase^{1–4}, the minimal components of active telomerase include the catalytic telomerase reverse transcriptase (TERT) and a noncoding RNA (*TERC*) that encodes the template to synthesize telomeric DNA⁵. Telomere homeostasis mediated by telomerase maintains genomic stability and regulates cell lifespan⁶. Mutations in TERT, *TERC* or dyskerin, a telomerase-associated nucleolar protein involved in ribosomal RNA maturation⁷, are found in dyskeratosis congenita, a syndrome characterized by ectodermal dysplasia and bone marrow failure, and TERT mutations have been reported in aplastic anaemia and idiopathic pulmonary fibrosis⁸. Moreover, alterations in the regulation of telomeres and telomerase contribute to malignant transformation by affecting genomic integrity and cell immortalization⁶.

However, accumulating evidence suggests that TERT has activities beyond telomere maintenance^{9–13} and forms several intracellular complexes^{2–4}. In particular, the overexpression of TERT induces increased tumour susceptibility^{9,10} and disrupts stem-cell function independently of telomere maintenance¹², whereas the suppression of TERT expression alters global chromatin structure¹¹. Indeed, some of these telomere-independent functions of TERT do not require the expression of *TERC*¹².

Identification of a second RNA that interacts with TERT

To identify human TERT partners, we stably overexpressed a tandem affinity peptide (TAP)-tagged TERT protein in HeLa S3 cells, isolated TERT immune complexes, and identified a heterogeneous mixture of 38 RNA sequences associated with TERT (Supplementary Fig. 2 and Supplementary Table 1). We found that 5% of the sequences corresponded to *TERC* and the RNA component of mitochondrial RNA processing endoribonuclease (*RMRP*). *RMRP* is a 267-nucleotide noncoding RNA that is a small nucleolar RNA, like *TERC*, and is also found in mitochondria^{8,14}. *RMRP* mutations are found in the pleiotropic inherited syndrome, cartilage–hair hypoplasia¹⁵.

From a single immune complex, we confirmed that either overexpressed or endogenous TERT interacts with *RMRP* and *TERC*, by

isolating TAP–TERT (Fig. 1a) or endogenous TERT (Fig. 1b) complexes in both HeLa and 293T cells under conditions in which we failed to recover the ribozyme *RNase P*. We also found that the abundance of TERT–*RMRP* and TERT–*TERC* complexes was similar, even though *TERC* was expressed at five-fold higher levels than *RMRP* in these cells (Fig. 1c and Supplementary Fig. 3).

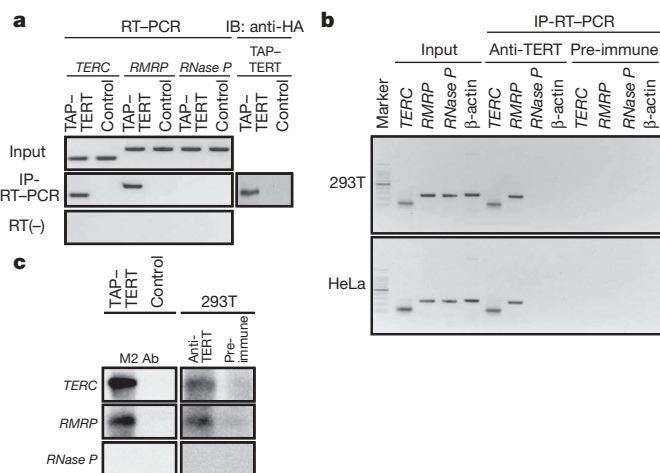


Figure 1 | TERT and *RMRP* interact. **a**, Detection of *RMRP* and *TERC*. RNA species associated with TAP–TERT complexes from a single immunoprecipitation (IP) were isolated and subjected to PCR with reverse transcription (RT–PCR). RT (–) indicates the absence of reverse transcriptase. Right panel shows the levels of TAP–TERT. HA, haemagglutinin; IB, immunoblot. **b**, TERT interacts with endogenous *RMRP*. TERT complexes from 293T and HeLa cells were isolated with an anti-TERT antibody and associated RNAs were subjected to RT–PCR. **c**, RNAs purified from TERT complexes isolated from HeLa S3 cells expressing TAP–TERT or a control vector or 293T cells were subjected to northern blotting. Ab, antibody.

¹Cancer Stem Cell Project, National Cancer Center Research Institute, 5-1-1 Tsukiji, Chuo-ku, Tokyo 104-0045, Japan. ²RIKEN Omics Science Center, RIKEN Yokohama Institute, 1-7-22 Suehiro-cho, Tsurumi-ku, Yokohama 230-0045, Japan. ³Department of Medical Oncology, Dana-Farber Cancer Institute and Departments of Medicine, Brigham and Women's Hospital and Harvard Medical School, 44 Binney Street, Boston, Massachusetts 02115, USA. ⁴Broad Institute of Harvard and MIT, 7 Cambridge Center, Cambridge, Massachusetts 02142, USA. ⁵PREST, Japan Science and Technology Agency, 4-1-8 Honcho Kawaguchi, Saitama 332-0012, Japan.

To characterize the interaction between TERT and *RMRP*, we used TERT truncation mutants and found that the amino terminal end of TERT (1–531) was necessary for interactions with *RMRP* (Supplementary Fig. 4). This region overlaps with two regions required for the binding of *TERC*^{8,16}. These observations demonstrate that TERT and *RMRP* form a new ribonucleoprotein complex distinct from the TERT–*TERC* enzyme.

The TERT–*RMRP* complex has RdRP activity

To test whether *RMRP* substitutes for *TERC* to reconstitute telomerase activity, we combined recombinant TERT with *TERC* or *RMRP* RNAs transcribed *in vitro*. Although we detected telomerase activity with TERT and *TERC* (Supplementary Fig. 5), we failed to detect telomerase activity when TERT and *RMRP* were co-incubated.

TERT has also been shown to act as a terminal transferase¹⁷, and human TERT shares sequence similarity to both viral reverse transcriptases and RdRPs¹⁸. RdRPs participate in the endogenous RNA interference (RNAi) pathway and in the regulation of post-transcriptional gene silencing^{19–23}. To examine whether the TERT–*RMRP* complex has RdRP and/or terminal transferase activity, we established an RNA synthesis activity assay with recombinant TERT protein (Supplementary Fig. 6) and RNA molecules transcribed *in vitro*. We predicted three modes that the TERT–*RMRP* complex might use to elongate RNA: (1) as an RdRP that uses a *de-novo*-synthesized RNA primer to elongate a complementary strand (Fig. 2a, left panel); (2) as an RdRP that uses a 3' fold-back (back-priming) configuration of template RNA as a primer (Fig. 2a, middle panel); or (3) as a terminal transferase (Fig. 2a, right panel). Viral RdRPs^{24,25} have been shown to use the first two modes to prime RdRP activity, and cellular RdRPs in

fission yeast²⁶ and fungi²³ use similar priming mechanisms to produce double-stranded (ds) RNAs that act as precursors for RNAi.

We found that recombinant TERT and *RMRP* produced two different products depending on the salt concentration (Fig. 2b and Supplementary Fig. 7). Specifically, we found ~267-nucleotide- (corresponding to sense *RMRP*) and ~534-nucleotide-sized products (hereafter referred to as sense plus antisense *RMRP* products) under high salt conditions, and *RMRP*-sized products under low salt conditions. To discriminate between these modes, we treated the products of the RdRP assay with RNase T1 (Fig. 2c) using conditions that favour the digestion of single-stranded RNA. RNase T1 treatment eliminated the ~267-nucleotide *RMRP*-sized RNA products produced under low salt concentrations (data not shown), indicating that [³²P]UTP was incorporated by terminal transferase activity.

In contrast, under high salt conditions, we found two RNAs (~267 and ~534 nucleotides) that collapsed into a single ~267-nucleotide band after treatment with RNase T1 (Fig. 2c). To eliminate the possibility that the sense plus antisense product represented partially denatured RNAs, we treated the products of the RdRP assay with bacterial RNase III to digest dsRNA, and found that only the input ~267-nucleotide RNA remained (Fig. 2d). Furthermore, when we left out adenine or guanine ribonucleotides, we failed to detect the sense plus antisense product (Fig. 2e). These observations confirm that the ~534-nucleotide sense plus antisense products are formed by RdRP activity and represent a double-stranded hairpin structure created by an RNA molecule composed of sense and antisense strands of *RMRP*.

To confirm that the interaction between TERT and *RMRP* was required for RdRP activity, we performed an RdRP activity assay using

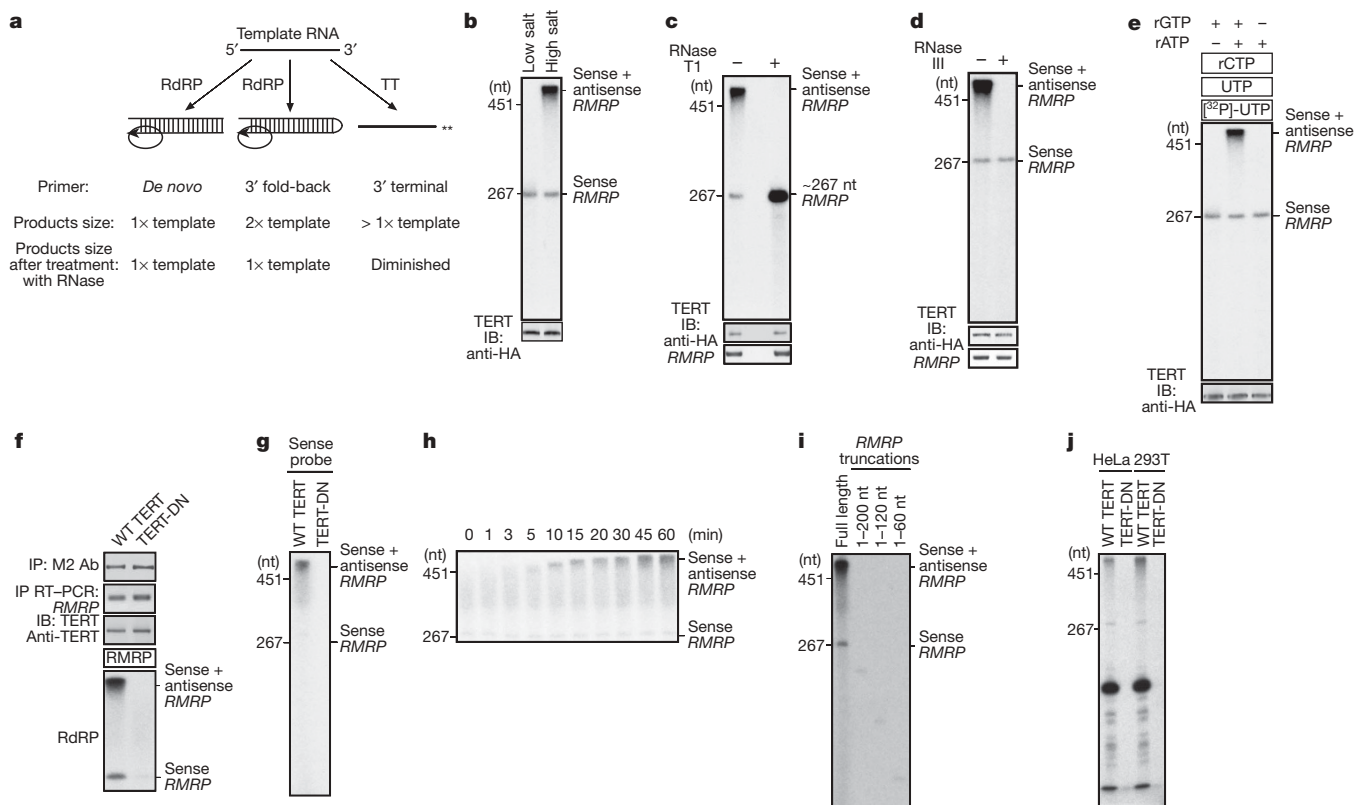


Figure 2 | TERT and *RMRP* have RdRP activity. **a**, Predicted RNA products produced by RdRP or terminal transferase (TT) activity. **b**, RNA products produced by the RdRP activity derived from recombinant TERT and *RMRP*. **c**, Treatment of RNA products with RNase T1 (**c**) or bacterial RNase III (**d**). **e**, RdRP assay performed in the presence of ribonucleotides (middle) or in the absence of adenine (left lane) or guanine (right lane) ribonucleotides. A and G are present within the first 5 nucleotides of the predicted complementary strand of *RMRP*. **f**, TERT-DN binds *RMRP* but lacks RdRP activity. TERT immune complexes were

isolated from 293T cells expressing Flag-tagged TERT or Flag-tagged TERT-DN. RdRP activity is shown in the bottom panel. WT, wild-type. **g**, Northern blotting to detect complementary sequence of *RMRP*. **h**, Time course of RdRP activity. **i**, RNA products produced by recombinant TERT and truncation mutants of *RMRP* transcribed *in vitro*. Faint signals at 200, 120 and 60 nucleotides are TERT terminal transferase products. **j**, RNA products produced by the RdRP activity derived from recombinant TERT or TERT-DN and total RNA. A limited pool of RNAs serves as template for RdRP activity.

combinations of recombinant mutant TERT proteins and *RMRP*. We failed to detect RdRP reaction products when TERT and *TERC* were co-incubated (Supplementary Fig. 8). Moreover, when we used the TERT-HT1 mutant that does not bind *RMRP* (Supplementary Fig. 4), we failed to observe labelled RNA products (Supplementary Fig. 8) under conditions in which we detected two different RNA products in reactions containing wild-type TERT and *RMRP*. We previously described a catalytically inactive TERT mutant (TERT-DN) that fails to elongate telomeres^{11,27}. We confirmed that the recombinant TERT-DN mutant retained the ability to bind *RMRP* (Fig. 2f), but that the TERT-DN-*RMRP* complex lacked detectable RdRP activity (Fig. 2f). Thus TERT acts as the catalytic subunit for both the telomerase reverse transcriptase and RdRP activities.

TERT-*RMRP* RdRP produces dsRNA

These observations suggest that the TERT-*RMRP* RdRP synthesizes dsRNA in a template-dependent manner. To confirm the synthesis of the *RMRP* complementary strand, we used the sense strand of *RMRP* as a probe in northern blotting. We detected the antisense strand of *RMRP* in reactions containing recombinant wild-type TERT protein and *RMRP*, but not in reactions containing TERT-DN and *RMRP* (Fig. 2g). Furthermore, we detected the sense plus antisense product in the RdRP assay using the antisense strand of *RMRP* as a probe (Supplementary Fig. 9). These observations indicate that the TERT-*RMRP* RdRP produces dsRNAs in a template-dependent manner *in vitro*.

To determine whether the TERT-*RMRP* RdRP uses a back-priming mechanism, we examined the priming process using TERT and *RMRP* as a model system and found that elongation products appeared in a time-dependent manner (Fig. 2h and Supplementary Fig. 10). To assess whether the *RMRP* RNA forms a 3' fold-back configuration, we generated 3' *RMRP* truncation mutants and failed to find any reaction products (Fig. 2i). Thus, unlike what has been described for other cellular RdRPs, the TERT-*RMRP* RdRP has a restricted preference for RNA molecules that can be used as a template. Indeed, when we incubated purified recombinant TERT together with total cellular RNA and [³²P]UTP, we identified a limited number of labelled RNAs (Fig. 2j). Although the secondary structure adopted by *RMRP* to create the 3' fold-back is not known, these observations suggest that *RMRP* can itself serve as a primer for the polymerization process using a 3' fold-back structure.

To ascertain whether this RdRP activity also occurs *in vivo*, we used the sense strand of *RMRP* as a probe and found ~534-nucleotide RNAs that contain antisense *RMRP* in RNA derived from 293T, HeLa and MCF7 cells (Fig. 3a and Supplementary Figs 11 and 12). Moreover, we detected sense products and sense plus antisense products using *RMRP* antisense-strand probe (Fig. 3b). These observations confirmed that the ~534-nucleotide products contain both sense and antisense *RMRP* sequences. To determine whether TERT was necessary for the appearance of antisense *RMRP* in cells, we examined the levels of the complementary *RMRP* strand in cells that do not express TERT and *TERC* (VA-13 cells)²⁸, in cells that transiently express low levels of TERT (BJ cells)^{27,29,30}, and in cells that constitutively express TERT (293T and HeLa cells). We also introduced a control vector or a vector that encodes TERT in VA-13 and BJ cells. We detected the complementary *RMRP* strand using a quantitative RNase protection assay with a sense-strand probe that detects antisense *RMRP* (Fig. 3c and Supplementary Fig. 13), and using northern blotting with both sense and antisense strand-specific *RMRP* probes (Fig. 3d and Supplementary Fig. 11a). The levels of antisense *RMRP* correlated with the expression of TERT (Fig. 3c, d). These observations confirmed that the TERT-*RMRP* RdRP produces double-stranded *RMRP* *in vivo*.

Effects of the TERT-*RMRP* complex on *RMRP* expression

To assess the consequences of overexpressing the TERT-*RMRP* complex on *RMRP* levels, we introduced *RMRP* into cells that lack TERT

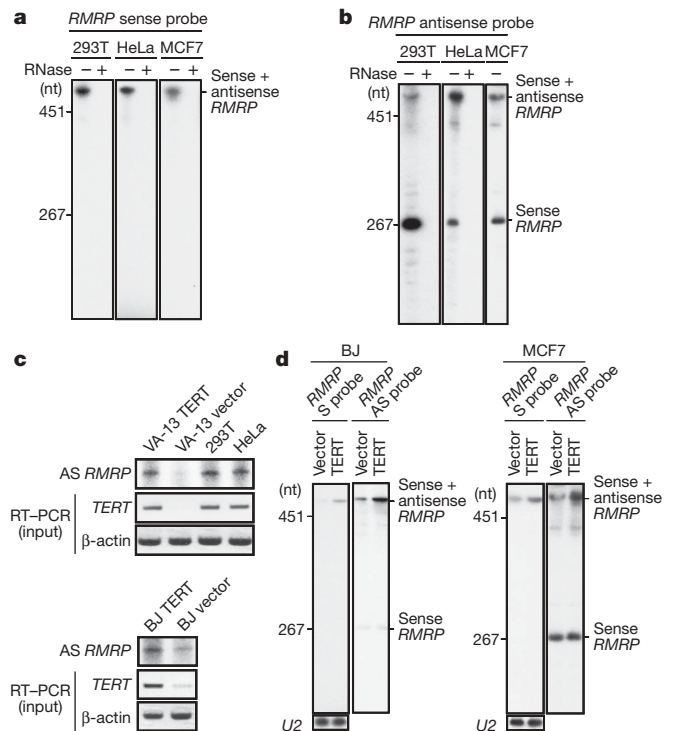


Figure 3 | Identification of dsRNA synthesized by the TERT-*RMRP* RdRP. **a**, Northern blotting to detect complementary sequence of *RMRP* in cell lines. '+' indicates samples treated with RNase. **b**, Northern blotting to detect the *RMRP* sense strand. **c**, TERT expression correlates with the levels of antisense (AS) *RMRP* detected by RNase protection assay. Vector denotes cells infected with a control vector. **d**, TERT expression correlates with the levels of the sense (S) plus antisense *RMRP* products detected by northern blotting. The bottom panel shows levels of the small nuclear RNA *U2*.

expression (VA-13), that transiently express TERT in a cell-cycle-dependent manner (BJ fibroblasts), and that constitutively express TERT (VA-13 and BJ fibroblasts expressing ectopic TERT, and HeLa and MCF7 cells). After expressing *RMRP* in cells lacking TERT (VA-13), we found that *RMRP* levels were increased (Fig. 4a and Supplementary Fig. 14). In contrast, in cells that express TERT, we found that the steady-state levels of *RMRP* were decreased when *RMRP* was overexpressed, regardless of the promoter that was used to express *RMRP* (Fig. 4a and Supplementary Fig. 14). We also found that forced TERT expression in VA-13 or BJ cells suppressed *RMRP* expression (Fig. 4b and Supplementary Fig. 15). Consistent with these findings, suppression of TERT in HeLa cells led to increased *RMRP* expression (Fig. 4c).

Because the 3' end of *RMRP* was essential for TERT-*RMRP* activity (Fig. 2i), we examined the effects of expressing *RMRP* truncation mutants lacking 3' ends and found that only truncation mutants lacking intact 3' ends were readily overexpressed (Fig. 4d). These observations demonstrate that *RMRP* expression levels are dependent on the TERT-*RMRP* RdRP and suggest that *RMRP* levels are controlled by an RdRP-dependent, negative-feedback mechanism.

Identification of siRNAs derived from *RMRP*

In other organisms, RdRPs synthesize dsRNAs that are processed into active short interfering RNAs (siRNAs)³¹. Because manipulating TERT and *RMRP* levels affected *RMRP* expression, we proposed that the TERT-*RMRP* complex produces *RMRP*-specific siRNA to regulate *RMRP* levels. To test this possibility, we used sense and antisense probes corresponding to *RMRP* (nucleotides 21–40) in northern blotting and found double-stranded 22-nucleotide RNAs (Fig. 4e and Supplementary Fig. 11b). Because siRNAs contain 5' monophosphate and 3' hydroxyl groups^{32–34}, we characterized the chemical

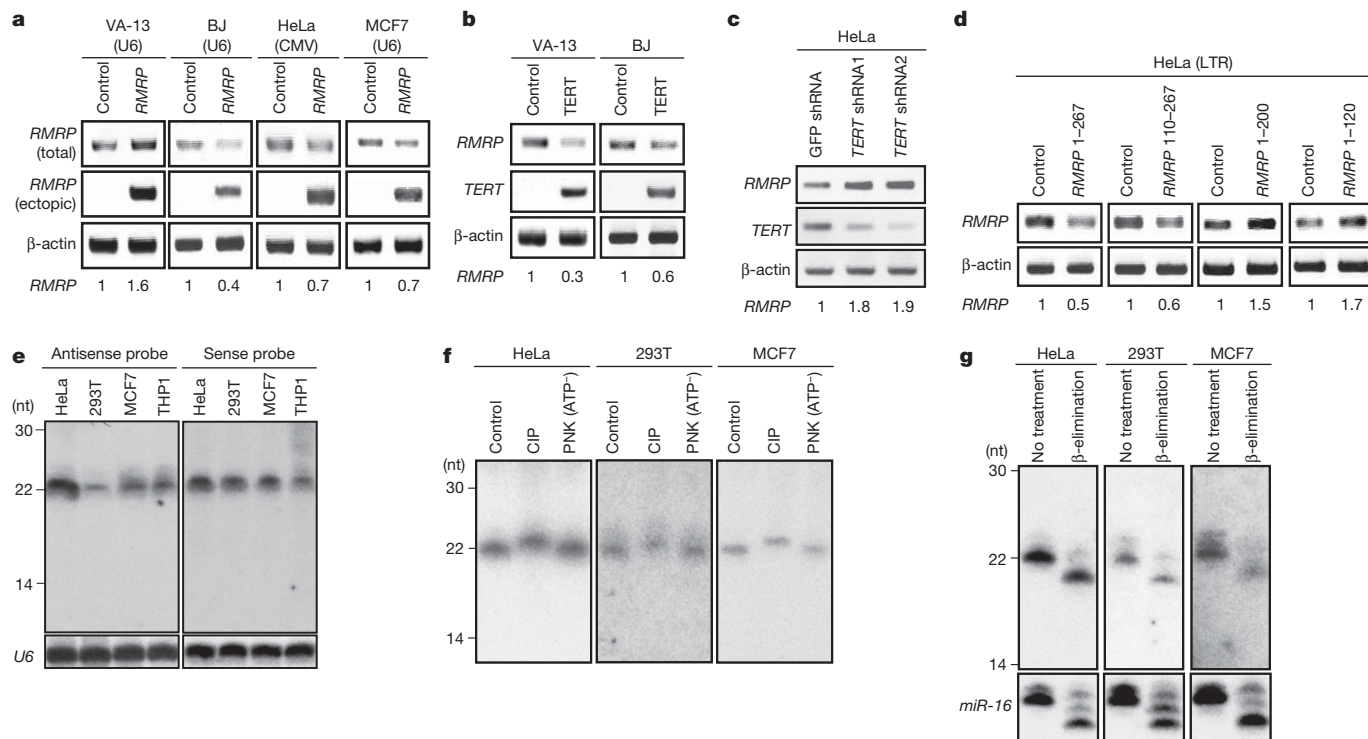


Figure 4 | Effects of dsRNA produced by the TERT–RMRP RdRP. **a**, Semi-quantitative RT–PCR for total *RMRP* and retrovirally delivered *RMRP* (ectopic) in cell lines expressing control or *RMRP* expression vectors. Promoters to express *RMRP* are indicated. The relative intensity of *RMRP* is noted below each panel. CMV, cytomegalovirus. See Supplementary Fig. 14. **b**, RT–PCR for total *RMRP*. See Supplementary Fig. 15. **c**, Effects of suppressing TERT on *RMRP* levels. A control shRNA (green fluorescent protein (GFP) shRNA) or two different *TERT*-specific shRNAs were stably introduced into HeLa cells. **d**, Effects of *RMRP* mutants on

RMRP levels. LTR, long terminal repeat. RT–PCR was used to detect *RMRP* levels in **c** and **d**. **e**, Detection of small RNA species in human cells. Northern blotting to detect small RNAs (22 nucleotides in length) using antisense (left panel) and sense (right panel) probes derived from nucleotides 21–40 of *RMRP*. **f**, **g**, Analysis of the termini of the small RNA species identified in **e**. Total RNA was incubated with the indicated enzyme (**f**), or oxidation- β -elimination reactions (**g**) were performed. Northern blotting was performed with antisense probe. CIP, calf intestinal phosphatase; PNK, polynucleotide kinase. ATP- indicates samples lacking ATP.

nature of the small RNA ends. We found that calf intestinal phosphatase slowed the migration of these short RNAs, and subsequent incubation with polynucleotide kinase and ATP restored the mobility of the short RNAs, indicating that either the 5' or the 3' end of this small RNA is monophosphorylated (Fig. 4f and data not shown). Moreover, incubation with polynucleotide kinase in the absence of ATP did not alter the migration (Fig. 4f), and oxidation and β -elimination treatment increased the migration of these small RNAs (Fig. 4g), indicating that the 3' ends bear vicinal 2',3' dihydroxyls. Together, these observations confirm that these small RNAs contain 5' monophosphate and 3' hydroxyl groups, and therefore share the size and chemical composition of known siRNAs.

To demonstrate that dsRNAs produced by the TERT–RMRP RdRP are processed into siRNA, we suppressed the expression of *Dicer* with two distinct *Dicer*-specific short hairpin RNAs (shRNAs). Suppression of *Dicer* to levels that partially inhibited the processing of the microRNA *miR-16* (Fig. 5a and Supplementary Fig. 16) led to diminished levels of the siRNAs derived from *RMRP* (Fig. 5a). When we suppressed *Dicer* expression in HeLa, 293T or MCF7 cells, we found that endogenous *RMRP* levels increased up to 3.7-fold (Fig. 5b). Suppressing *Dicer* expression in VA-13 cells that lack TERT did not affect the levels of single-stranded *RMRP* (Fig. 5b), but did increase levels of the elongated sense plus antisense *RMRP* products in cells that constitutively express TERT (Supplementary Fig. 17). Moreover, we found that only the sense strands of these endogenous *RMRP*-specific siRNAs were associated with human AGO2 (also known as EIF2C2; Fig. 5c). These observations indicate that the endogenous *RMRP*-specific siRNAs are processed by the RNA-induced silencing complex, similar to other small RNAs that are processed into siRNA.

To confirm that these small RNAs act as siRNAs, we identified small RNAs from total RNA that hybridized to probes spanning *RMRP*, synthesized siRNA corresponding to the identified sequences, and tested the consequences of introducing this siRNA in HeLa, 293T and MCF7 cells. We found that the synthesized siRNA suppressed endogenous *RMRP* levels (Supplementary Fig. 18). These observations provide evidence that similar to other cellular RdRPs, the TERT–RMRP RdRP synthesizes dsRNAs that act as a precursor for siRNAs.

Discussion

Here we demonstrate that human TERT and *RMRP* form a distinct ribonucleoprotein complex that has the ability to produce dsRNAs (Supplementary Fig. 1). Like RdRPs found in other organisms, the human TERT–RMRP complex produces dsRNAs that act as substrates for the generation of siRNA. However, unlike other cellular RdRPs^{23,26,31,35,36}, the human TERT–RMRP RdRP shows a strong preference for RNA templates that can form 3' fold-back structures. Because other cellular RdRPs have been identified using assays that require primer-independent RdRP activity^{23,26,36}, the substrate specificity of the human TERT–RMRP RdRP may, in part, account for the difficulty in identifying mammalian enzymes that have RdRP activity.

Although the cellular RdRPs described until now do not show a primer requirement, several viral RdRPs use both primer-dependent and primer-independent mechanisms, and fungal and yeast RdRPs are also able to use a back-priming mechanism^{23,26}. Because TERT is a closed right-handed polymerase³⁷ evolutionarily related to both reverse transcriptases and viral RdRPs¹⁸, these observations are consistent with previous observations that indicate that right-handed RdRPs exhibit primer-dependent RdRP polymerase activity³⁸.

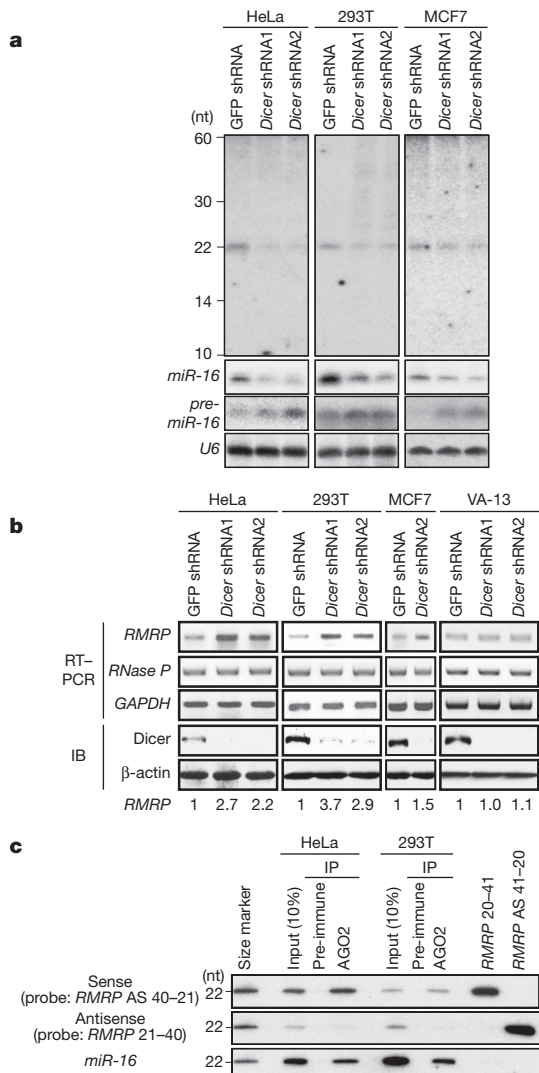


Figure 5 | Production of RMRP-derived endogenous siRNAs depends on Dicer. **a**, Effect of suppressing *Dicer* on RMRP-derived small RNAs. Northern blotting was performed to detect: (1) small RNAs using the antisense strand of RMRP as a probe in the indicated cells expressing control shRNA (GFP shRNA) or *Dicer*-specific shRNAs (*Dicer* shRNA1 and shRNA2); (2) precursor microRNA *pre-miR-16* and mature *miR-16* using a *miR-16*-specific probe; and (3) *U6* RNA. See Supplementary Fig. 16. **b**, RT-PCR for total RMRP from cell lines expressing control shRNA or *Dicer*-specific shRNAs. IB, immunoblot. The relative intensity of RMRP is noted at the bottom of the panel. **c**, RMRP-derived small RNAs are associated with AGO2. Human AGO2 immune complexes were isolated using anti-AGO2-specific antisera or pre-immune sera, and small RNAs were detected by northern blotting. Blotting of oligonucleotides (RMRP 20–41 and RMRP AS 41–20) is also shown.

Using RMRP as a template, the TERT–RMRP RdRP produces dsRNAs that are processed by Dicer into 22-nucleotide dsRNAs that contain 5' monophosphate and 3' hydroxyl groups and are loaded into AGO2, confirming that these short RNAs represent endogenous siRNAs. Recent work has shown that in oocytes and embryonic stem cells, endogenous siRNA can also be formed by the transcription of complementary sense and antisense strands^{39–41}. Thus, in mammals at least two mechanisms lead to the production of dsRNAs that are processed into siRNA. Further work will be necessary to determine whether there are tissue-dependent differences in the use of these two mechanisms and whether other mammalian RdRPs exist.

We found that the TERT–RMRP RdRP regulates RMRP levels by a negative-feedback control mechanism. The identities and functions

of the RNAs other than RMRP that act as templates for the TERT–RMRP RdRP remain to be identified (Fig. 2j). However, because endogenously encoded siRNAs suppress L1 retrotransposition in human cells⁴², these observations suggest that the TERT–RMRP complex may regulate the expression of other genes by generating siRNAs.

Because mutations in RMRP are found in cartilage–hair hypoplasia¹⁵, these findings suggest that perturbation of the TERT–RMRP complex is involved in the pathogenesis of this disorder. The involvement of human TERT in two syndromes characterized by stem-cell failure (cartilage–hair hypoplasia and dyskeratosis congenita)^{7,8,43} suggests that ribonucleoprotein complexes containing TERT has a critical role in stem cell biology. Indeed, overexpression of mouse TERT in mice lacking *Terc* leads to defects in normal hair follicle stem-cell function¹² at least in part by altering gene expression programs related to stem cell function⁴⁴. In mammals, TERT may regulate both telomere biology and gene expression through these two ribonucleoprotein complexes.

METHODS SUMMARY

RNAs that bind TERT were identified from HeLa S3 cells expressing a TAP epitope-tagged TERT. RNAs that bound to TERT after two rounds of purification were analysed using an Experion capillary electrophoresis device (Bio-Rad) to visualize RNA species. For RNA cloning and sequencing, the same samples were separated using a 7 M urea/15% polyacrylamide gel, and RNAs recovered from the gel were cloned using a small RNA cloning Kit (TaKaRa). Purified glutathione S-transferase (GST)–TERT was isolated from *Escherichia coli* and incubated with either *TERC* or RMRP transcribed *in vitro*, to assess the ability of such complexes to exhibit telomerase or RdRP activity. RNAi was used to suppress TERT and to show that the TERT–RMRP complex also produces dsRNA in cells. Northern blotting with sense and antisense probes specific for RMRP (nucleotides 21–40) identified 22-nucleotide, double-stranded RNAs that contained a 5' monophosphate and a 3' hydroxyl group, which were loaded into human AGO2. To determine the function of these RMRP-derived small RNAs, a chemically synthesized siRNA corresponding to these small RNAs (siRNA: 5'-GGCTACACACTGAGGACTC-3'; Dharmacon) was transfected into HeLa, 293T and MCF7 cells.

Full Methods and any associated references are available in the online version of the paper at www.nature.com/nature.

Received 28 May; accepted 10 July 2009.

Published online 23 August 2009.

- Cohen, S. B. *et al.* Protein composition of catalytically active human telomerase from immortal cells. *Science* **315**, 1850–1853 (2007).
- Fu, D. & Collins, K. Purification of human telomerase complexes identifies factors involved in telomerase biogenesis and telomere length regulation. *Mol. Cell* **28**, 773–785 (2007).
- Venteicher, A. S., Meng, Z., Mason, P. J., Veenstra, T. D. & Artandi, S. E. Identification of ATPases pontin and reptin as telomerase components essential for holoenzyme assembly. *Cell* **132**, 945–971 (2008).
- Venteicher, A. S. *et al.* A human telomerase holoenzyme protein required for Cajal body localization and telomere synthesis. *Science* **323**, 644–648 (2009).
- Weinrich, S. L. *et al.* Reconstitution of human telomerase with the template RNA component hTR and the catalytic protein subunit hTRT. *Nature Genet.* **17**, 498–502 (1997).
- Chan, S. W. & Blackburn, E. H. New ways not to make ends meet: telomerase, DNA damage proteins and heterochromatin. *Oncogene* **21**, 553–563 (2002).
- Liu, J. M. & Ellis, S. R. Ribosomes and marrow failure: coincidental association or molecular paradigm? *Blood* **107**, 4583–4588 (2006).
- Calado, R. T. & Young, N. S. Telomere maintenance and human bone marrow failure. *Blood* **111**, 4446–4455 (2008).
- Gonzalez-Suarez, E. *et al.* Increased epidermal tumors and increased skin wound healing in transgenic mice overexpressing the catalytic subunit of telomerase, mTERT, in basal keratinocytes. *EMBO J.* **20**, 2619–2630 (2001).
- Artandi, S. E. *et al.* Constitutive telomerase expression promotes mammary carcinomas in aging mice. *Proc. Natl Acad. Sci. USA* **99**, 8191–8196 (2002).
- Masutomi, K. *et al.* The telomerase reverse transcriptase regulates chromatin state and DNA damage responses. *Proc. Natl Acad. Sci. USA* **102**, 8222–8227 (2005).
- Sarin, K. Y. *et al.* Conditional telomerase induction causes proliferation of hair follicle stem cells. *Nature* **436**, 1048–1052 (2005).
- Lee, J. *et al.* TERT promotes cellular and organismal survival independently of telomerase activity. *Oncogene* **27**, 3754–3760 (2008).

14. Tollervey, D. & Kiss, T. Function and synthesis of small nucleolar RNAs. *Curr. Opin. Cell Biol.* **9**, 337–342 (1997).
15. Ridanpaa, M. *et al.* Mutations in the RNA component of RNase MRP cause a pleiotropic human disease, cartilage-hair hypoplasia. *Cell* **104**, 195–203 (2001).
16. Moriarty, T. J., Huard, S., Dupuis, S. & Autexier, C. Functional multimerization of human telomerase requires an RNA interaction domain in the N terminus of the catalytic subunit. *Mol. Cell. Biol.* **22**, 1253–1265 (2002).
17. Lue, N. F. *et al.* Telomerase can act as a template- and RNA-independent terminal transferase. *Proc. Natl Acad. Sci. USA* **102**, 9778–9783 (2005).
18. Nakamura, T. M. *et al.* Telomerase catalytic subunit homologs from fission yeast and human. *Science* **277**, 955–959 (1997).
19. Mourrain, P. *et al.* *Arabidopsis* *SGS2* and *SGS3* genes are required for posttranscriptional gene silencing and natural virus resistance. *Cell* **101**, 533–542 (2000).
20. Smardon, A. *et al.* EGO-1 is related to RNA-directed RNA polymerase and functions in germ-line development and RNA interference in *C. elegans*. *Curr. Biol.* **10**, 169–178 (2000).
21. Lipardi, C., Wei, Q. & Paterson, B. M. RNAi as random degradative PCR: siRNA primers convert mRNA into dsRNAs that are degraded to generate new siRNAs. *Cell* **107**, 297–307 (2001).
22. Sijen, T. *et al.* On the role of RNA amplification in dsRNA-triggered gene silencing. *Cell* **107**, 465–476 (2001).
23. Makeyev, E. V. & Bamford, D. H. Cellular RNA-dependent RNA polymerase involved in posttranscriptional gene silencing has two distinct activity modes. *Mol. Cell* **10**, 1417–1427 (2002).
24. Semler, B. L. & Wimmer, E. *Molecular Biology of Picornaviruses* 255–267 (American Society for Microbiology, 2002).
25. Behrens, S. E., Tomei, L. & De Francesco, R. Identification and properties of the RNA-dependent RNA polymerase of hepatitis C virus. *EMBO J.* **15**, 12–22 (1996).
26. Sugiyama, T., Cam, H., Verdel, A., Moazed, D. & Grewal, S. I. RNA-dependent RNA polymerase is an essential component of a self-enforcing loop coupling heterochromatin assembly to siRNA production. *Proc. Natl Acad. Sci. USA* **102**, 152–157 (2005).
27. Masutomi, K. *et al.* Telomerase maintains telomere structure in normal human cells. *Cell* **114**, 241–253 (2003).
28. Ford, L. P. *et al.* Telomerase can inhibit the recombination-based pathway of telomere maintenance in human cells. *J. Biol. Chem.* **276**, 32198–32203 (2001).
29. Pascale, E., Cimino Reale, G. & D'Ambrosio, E. Tumor cells fail to *trans*-induce telomerase in human umbilical vein endothelial cell cultures. *Cancer Res.* **64**, 7702–7705 (2004).
30. Won, J., Chang, S., Oh, S. & Kim, T. K. Small-molecule-based identification of dynamic assembly of E2F-pocket protein-histone deacetylase complex for telomerase regulation in human cells. *Proc. Natl Acad. Sci. USA* **101**, 11328–11333 (2004).
31. Almeida, R. & Allshire, R. C. RNA silencing and genome regulation. *Trends Cell Biol.* **15**, 251–258 (2005).
32. Schwarz, D. S., Hutvagner, G., Haley, B. & Zamore, P. D. Evidence that siRNAs function as guides, not primers, in the *Drosophila* and human RNAi pathways. *Mol. Cell* **10**, 537–548 (2002).
33. Schwarz, D. S., Tomari, Y. & Zamore, P. D. The RNA-induced silencing complex is a Mg²⁺-dependent endonuclease. *Curr. Biol.* **14**, 787–791 (2004).
34. Vagin, V. V. *et al.* A distinct small RNA pathway silences selfish genetic elements in the germline. *Science* **313**, 320–324 (2006).
35. Nishikura, K. A short primer on RNAi: RNA-directed RNA polymerase acts as a key catalyst. *Cell* **107**, 415–418 (2001).
36. Aoki, K., Moriguchi, H., Yoshioka, T., Okawa, K. & Tabara, H. *In vitro* analyses of the production and activity of secondary small interfering RNAs in *C. elegans*. *EMBO J.* **26**, 5007–5019 (2007).
37. Gillis, A. J., Schuller, A. P. & Skordalakes, E. Structure of the *Tribolium castaneum* telomerase catalytic subunit TERT. *Nature* **455**, 633–637 (2008).
38. Salgado, P. S. *et al.* The structure of an RNAi polymerase links RNA silencing and transcription. *PLoS Biol.* **4**, e434 (2006).
39. Tam, O. H. *et al.* Pseudogene-derived small interfering RNAs regulate gene expression in mouse oocytes. *Nature* **453**, 534–538 (2008).
40. Watanabe, T. *et al.* Endogenous siRNAs from naturally formed dsRNAs regulate transcripts in mouse oocytes. *Nature* **453**, 539–543 (2008).
41. Babiarz, J. E., Ruby, J. G., Wang, Y., Bartel, D. P. & Blelloch, R. Mouse ES cells express endogenous shRNAs, siRNAs, and other Microprocessor-independent, Dicer-dependent small RNAs. *Genes Dev.* **22**, 2773–2785 (2008).
42. Yang, N. & Kazanian, H. H. Jr. L1 retrotransposition is suppressed by endogenously encoded small interfering RNAs in human cultured cells. *Nature Struct. Mol. Biol.* **13**, 763–771 (2006).
43. Guggenheim, R., Somech, R., Grunebaum, E., Atkinson, A. & Roifman, C. M. Bone marrow transplantation for cartilage-hair-hypoplasia. *Bone Marrow Transplant* **38**, 751–756 (2006).
44. Choi, J. *et al.* TERT promotes epithelial proliferation through transcriptional control of a Myc- and Wnt-related developmental program. *PLoS Genet.* **4**, e10 (2008).

Supplementary Information is linked to the online version of the paper at www.nature.com/nature.

Acknowledgements We thank T. Sugimura and S. Hirohashi at the National Cancer Center for comments. We also thank H. Siomi, H. Tabara and Y. Tomari for discussions. This work was supported in part by Grant-in-Aid for Young Scientists (A) 19689010 (K.M.) and Grant-in-Aid for Young Scientists (B) 19791141 (Y.M.) from the Ministry of Education, Culture, Sports, Science and Technology, by the Third-Term Comprehensive Control Research for Cancer (K.M.) from the Ministry of Health, Labor, and Welfare, by a Takeda Science Foundation grant (K.M.), the Uehara Memorial Foundation (K.M.), a J&J Focused Funding Award (W.C.H.) and R01 AG23145 from the National Institutes of Health (W.C.H.).

Author Contributions Y.M., M.Y., M.F., N.O., R.P. and V.K. performed experiments. T.L. and Y.H. designed and carried out the bioinformatics analyses of TERT-associated RNAs. Y.M., M.Y., W.C.H. and K.M. designed the experiments and discussed the interpretation of the results. W.C.H. and K.M. cowrote the manuscript.

Author Information Reprints and permissions information is available at www.nature.com/reprints. Correspondence and requests for materials should be addressed to W.C.H. (william_hahn@dfci.harvard.edu) or K.M. (kmasutom@ncc.go.jp).

METHODS

Cell culture and stable expression of TAP–TERT. The human cell lines 293T, MCF7, HeLa, HeLa S3 and VA-13 were maintained in DMEM supplemented with 10% heat-inactivated FBS. BJ fibroblasts were cultured as described⁴⁵. Amphotropic retroviruses were created as described^{45,46} using the vectors pWZL-Blast-N-Flag/HA–TERT (for HeLa-S3-TAP–TERT), pBABE-puro or pBABE-puro-TERT. After infection, cells were selected with blasticidin S (10 µg ml⁻¹) for 5 days or with puromycin (2 µg ml⁻¹) for 3 days.

Purification of TERT complexes and cloning of RNAs. HeLa S3 cells (2 × 10⁸) expressing or lacking (control) TAP–TERT were lysed in 5 ml of lysis buffer A (20 mM Tris-HCl, pH 7.4, 150 mM NaCl, 0.5% NP-40, 0.1 mM dithiothreitol (DTT)) and incubated for 30 min on ice. The lysate was then pelleted by centrifugation (16,000g) for 20 min at 4 °C. The supernatant was incubated with anti-Flag (M2) antibody-conjugated agarose overnight at 4 °C. The beads were washed three times with lysis buffer A and eluted with 3× Flag peptide (150 ng µl⁻¹). The resulting elution was incubated with Protein A Sepharose beads and an anti-HA antibody (F7; Santa Cruz) for 4 h at 4 °C. The beads were washed three times with lysis buffer A, and RNA was isolated using TRIzol (Invitrogen). RNA samples prepared in this manner were analysed using an Experion capillary electrophoresis device (Bio-Rad) to visualize RNA species. For RNA cloning and the sequencing, the same samples were separated using a 7 M urea/15% polyacrylamide gel, and RNAs recovered from gel were cloned using a small RNA cloning Kit (TaKaRa).

RNA preparation for immunoprecipitation RT–PCR. RNA samples that were prepared from the HeLa S3 cells expressing TAP–TERT as described earlier were also subjected to RT–PCR. For immunoprecipitation of endogenous TERT complexes, cells (1 × 10⁸) were lysed in 600 µl of lysis buffer A, sonicated and pre-cleared with 15 µl of 50% slurry of Protein A Sepharose (Pierce) for 2 h at 4 °C. The pre-cleared total cell lysate was incubated with a rabbit polyclonal anti-TERT antibody (Rockland, 2 µl) for 3 h at 4 °C, followed by incubation with 30 µl of 50% slurry of Protein A Sepharose overnight at 4 °C. After binding, the beads were washed three times for 30 min with lysis buffer A. RNA derived from a single immunoprecipitation was isolated from the Protein A Sepharose using TRIzol (Invitrogen) followed by RT–PCR with primers specific for *TERC*, *RMRP* or *RNase P*. Although other RNAs also co-purified with human TERT (Supplementary Table 1), we failed to confirm the interaction of *Alu* sequences or the 5.8S ribosomal RNA on the Y chromosome with TERT (data not shown).

RT–PCR and quantitative RT–PCR. Either total cellular RNA or RNA from immunoprecipitation was isolated using TRIzol (Invitrogen) and subjected to RT–PCR. The following primers were used: *TERC* (43F, 5'-TCTAACCC TAACTGAGAAGGGCGT-3' and 163R, 5'-TGCTCTAGAATGAACGGTGGGA AGG-3'), *RMRP* (F5, 5'-TGCTGAAGGCCGTATCCT-3' and R257, 5'-TGAGAATGAGCCCCGTGT-3'), *RNase P* (F50, 5'-GTCACCTCCACTCC CATGTCC-3' and R318, 5'-AATTGGGTTATGAGGTCCC-3'), and the human β-actin gene (also known as *ACTB*) (5'-CAAGAGATGGCCACGGCTGCT-3' and 5'-TCCTTCTGCATCCTGTCCGCA-3'). The reverse transcription reaction was performed for 60 min at 42 °C using the recovered RNA, and PCR was immediately performed (22 cycles for 293T cells, and 26 cycles for HeLa cells: 94 °C, 30 s; 60 °C, 30 s; 72 °C, 30 s).

Quantitative RT–PCR (qRT–PCR) was performed with a LightCycler 480 II (Roche) according to the manufacturer's protocols. The expression levels of *RMRP* were detected using the following primers and probe; forward primer, 5'-GAGAGTGCCACGTGCATACG-3', reverse primer, 5'-CTCAGCGGGATA-CGCTTCTT-3', VIC-labelled TaqMan MGB probe, 5'-ACGTAGACATT-CCCC-3'. β-actin was used as a reference.

Total *RMRP* was detected using primers (F5, 5'-TGCTGAAGGCC TGTATCCT-3' and R257, 5'-TGAGAATGAGCCCCGTGT-3') that amplify both endogenous and ectopically introduced *RMRP*. In Fig. 4a, for VA-13, BJ and MCF7 cells, reverse transcription was performed using random hexamers (GE Healthcare) and ectopically expressed *RMRP* was detected with vector-specific primers (F5, 5'-TGCTGAAGGCCGTATCCT-3' and LKO.1-RT, 5'-ACTGCCATTTGTCTCGAGGT-3'). For HeLa cells, reverse transcription was performed with pQC3' (5'-AAGCGGCTTCGGCCAGTAACGTTA-3') and PCR was performed with the primers F5 (5'-TGCTGAAGGCCGTATCCT-3') and R257 (5'-TGAGAATGAGCCCCGTGT-3'). Northern blotting and qRT–PCR experiments (Supplementary Fig. 14) confirmed that the differences in *RMRP* levels that were observed using the RT–PCR conditions used in Fig. 4a accurately reflect *RMRP* levels. Signal intensity was measured with ImageJ software.

Telomerase activity reconstituted *in vitro* and TRAP assay. *In vitro* reconstitution of telomerase activity (telomere-specific reverse transcriptase activity) was performed as described previously⁵. In brief, recombinant TERT was expressed in the TnT T7-Coupled Reticulocyte Lysate System (Promega) following the

manufacturer's instructions. Purified *TERC* or *RMRP* was included in the *in vitro* transcription/translation reactions. The telomeric repeat amplification protocol (TRAP)^{45–47} was used to detect telomere-specific reverse transcriptase activity.

Affinity purification of recombinant GST–TERT fusion proteins. GST–TERT–HA, GST–TERT–HT1 and GST–TERT–DN in the pGENKZ expression vector⁴⁸ were provided by S. Murakami. Bacteria (BL21-Gold) containing these vectors were plated at 30 °C overnight and then a single colony was picked to inoculate liquid cultures, which were incubated at 37 °C overnight. Thereafter 1 ml of this culture was re-inoculated into 100 ml of Luria-Bertani medium, incubated at 37 °C for 4 h without isopropyl-β-D-thiogalactoside (IPTG) induction, collected by centrifugation, suspended in a lysis buffer (20 mM Tris-HCl, pH 7.4, 150 mM NaCl, 0.5% NP-40, 0.1 mM DTT, 10 mM phenylmethyl sulphonyl fluoride (PMSF), proteinase inhibitor (Nacalai Tesque)) and sonicated twice for 10 s at 4 °C. After centrifugation of the sonicated lysates, the supernatants were passed through DEAE-Sepharose, and the GST-fusion proteins were recovered using glutathione-Sepharose 4B beads. The resin was washed with lysis buffer A at least three times, and the GST-fusion proteins were then eluted with glutathione at 4 °C for 1 h (20 mM glutathione (reduced form)) in elution buffer (50 mM Tris-HCl, pH 8.8, 150 mM NaCl, 0.5% NP-40, 0.1 mM DTT, 10 mM PMSF, proteinase inhibitor (Nacalai Tesque)). Supplementary Fig. 6 shows that wild type and TERT–DN were produced at similar levels using this method and the effects of incubation time and IPTG on yield. The average yield for this method is 500 ng (5 ng µl⁻¹) of active form of TERT from 100 ml culture.

RdRP assay. The affinity purified recombinant GST–TERT fusion protein (10 ng) was incubated with 1 µg of full length *RMRP* RNA or truncated *RMRP* products (*RMRP* 1–200, *RMRP* 1–120 and *RMRP* 1–60 for Fig. 2i) transcribed *in vitro* (SP6) in 200 mM KCl, 50 mM Tris-HCl, pH 8.3, 10 mM DTT, 30 mM MgCl₂, 50 µM rATP, 50 µM rGTP, 50 µM rCTP and 2 µCi of [α -³²P]UTP at 32 °C for 2 h. To perform the experiments under low salt conditions, 20 µl of 0.2× SSC was then added to adjust final salt concentration to 15 mM NaCl and 1.5 mM sodium citrate, whereas 20 µl of 4× SSC was added to adjust final salt concentration to 300 mM NaCl and 30 mM sodium citrate to achieve high salt conditions. These mixtures were incubated at 37 °C for a further 1 h. Resulting products were treated with proteinase K to stop the reaction and purified with phenol–chloroform. To ensure that RNA products were completely denatured, we performed both conventional formamide treatment (with 95% formamide/20 mM EDTA gel-loading buffer at 95 °C for 5 min) and a further treatment with 1 M de-ionized glyoxal at 65 °C for 15 min.

To analyse double-stranded RNA produced by the TERT–*RMRP* complex, we performed this RdRP assay and treated the products with bacterial RNase III (*E. coli*, Ambion; 50 mM NaCl, 10 mM Tris-HCl, pH 7.9, 1 mM DTT, 10 mM MgCl₂) or RNase T1 (Roche; 50 mM Tris-HCl, pH 8.3, 300 mM NaCl and 30 mM sodium citrate).

Northern blotting. Total RNA and small RNAs (<200 nucleotides in length) were isolated using a mirVana miRNA Isolation Kit (Ambion) according to the manufacturer's protocol. Total RNA or small RNA (10 µg) was separated on denaturing polyacrylamide gels, then blotted onto Hybond-N+ membranes (GE Healthcare) using a Trans-Blot SD Semi-Dry Transfer Cell (Bio-Rad). Hybridization was performed in Church buffer (0.5 M NaHPO₄, pH 7.2, 1 mM EDTA and 7% SDS) containing 10⁶ c.p.m. ml⁻¹ of each ³²P-labelled probe for 14 h. The membranes were washed in 2× SSC, and the signals were detected by autoradiography.

Identification of short RNA species derived from *RMRP*. Using ten consecutive probes corresponding to the *RMRP* sequence, we found that the small RNAs derived from *RMRP* shown in Figs 4e–g and 5a were detected by probes containing the complementary sequences to nucleotides 21–40 of *RMRP*. To determine the function of these *RMRP*-derived small RNAs, we purchased a chemically synthesized siRNA targeting this 20-nucleotide portion of the *RMRP* sequence (siRNA: 5'-GGCTACACACTGAGGACTC-3'; Dharmacon) and transfected this siRNA into HeLa, 293T and MCF7 cells plated on six-well dishes using Lipofectamine 2000 (Invitrogen) according to the manufacturer's protocol.

RNase protection assay. *RMRP* RNA was transcribed with SP6 RNA polymerase in the presence of [α -³²P]UTP using RiboMAX Large Scale RNA Production System (Promega). Total cellular RNA (30 µg) was hybridized overnight at 60 °C with equal amounts of ³²P-labelled *RMRP* sense probe. Hybrids were digested with RNase A and RNase T1. The protected fragments were separated by PAGE under denaturing conditions and visualized by autoradiography.

Analysis of the chemical structure of the ends of small RNAs. To determine the phosphorylation status of the termini of small RNAs, 30 µg of small RNA (<200 nucleotides in length) was treated with calf intestinal alkaline phosphatase (CIP; TaKaRa) for 2 h at 37 °C. CIP was inactivated by phenol–chloroform extraction. Part of the CIP-treated RNA was then treated with T4 polynucleotide

kinase (TaKaRa) supplemented with 1 mM ATP for 2 h at 37 °C, and phenol–chloroform extraction was performed. Small RNA (15 µg) was treated with T4 polynucleotide kinase without ATP for 2 h at 37 °C. The reaction was inactivated by phenol–chloroform extraction. After overnight sodium acetate–ethanol precipitation at –20 °C, the treated RNAs were resolved by 20% denaturing polyacrylamide/urea gel electrophoresis and then analysed by northern blotting^{42,43}.

To further analyse the 3' end of these small RNAs, we performed oxidation and β-elimination reactions. Specifically, the NaIO₄ reaction was performed by adding 20 µg of small RNA in water to 5× borate buffer (148 mM borax and 148 mM boric acid, pH 8.6) and freshly dissolved 200 mM NaIO₄ to create a final concentration of 1× borate buffer and 25 mM NaIO₄. The mixtures were incubated for 10 min at 20 °C. Glycerol was added to quench remaining NaIO₄, and the samples were incubated for a further 10 min at 20 °C. For β-elimination, small RNAs were dried by centrifugation and evaporation and dissolved in 50 µl of 1× borax buffer (30 mM borax, 30 mM boric acid and 50 mM NaOH, pH 9.5) and incubated at 45 °C for 90 min. Nucleic acids were recovered by sodium acetate–ethanol precipitation at –20 °C overnight, and the treated RNAs were resolved by 20% denaturing 7 M urea PAGE and analysed by northern blotting⁴³.

Stable expression of shRNA. We used the pLKO.1-puro vector and the sequences described below to create shRNA vectors specific for *TERT*, *Dicer* and GFP. These vectors were used to make amphotropic retroviruses and polyclonal cell populations were purified with selection with puromycin (2 µg ml⁻¹). The sequences used for the indicated short hairpin RNAs are shown below where the capitalized letters represent the targeting sequences: *TERT* shRNA1, 5'-GGAAGACAGTGGTGAACCTCCctcgagGGAAGTTCACCACTGTCTCCttttt-3' and 5'-aattcaaaaaGGAAGACAGTGGTGAACCTCCctcgagGGAAGTTCACCACTGTCTCC-3'; *TERT* shRNA2, 5'-GGAACACCAAGAAGTTCATCTctcgagAGATGAACTTCTTGGTGTTCttttt-3' and 5'-aattcaaaaaGGA

ACACCAAGAAGTTCATCTctcgagAGATGAACTTCTTGGTGTTC-3'. *Dicer* sequences: *Dicer* shRNA1, 5'-GCTCGAAATCTTACGCAAATActcgagTATTTCGTAAGATTTTCGAGCttttt-3' and 5'-aattcaaaaaGCTCGAAATCTTACGCAATAActcgagTATTTCGTAAGATTTTCGAGC-3'; *Dicer* shRNA2, 5'-CCACA CATCTTCAAGACTTAActcgagTTAAGTCTTGAAGATGTGTGGttttt-3' and 5'-aattcaaaaaCCACACATCTTCAAGACTTAActcgagTTAAGTCTTGAAGATGTGTGG-3'.

Immunoprecipitation of human AGO2 complexes. HeLa or 293T cells were lysed in lysis buffer A and immunoprecipitation was performed using pre-immune sera or anti-AGO2 antibodies⁴⁹ (provided by H. Siomi and M. C. Siomi). RNA was isolated using TRIzol from the protein A beads and resolved by electrophoresis on 7 M urea 20% PAGE. Small RNAs were detected by northern blotting with an antisense probe, a sense probe derived from nucleotides 21–40 of *RMRP*, or a *miR-16*-specific probe (5'-CGCCAATATTTACGTGTGCTA-3').

45. Hahn, W. C. *et al.* Creation of human tumour cells with defined genetic elements. *Nature* **400**, 464–468 (1999).
46. Hahn, W. C. *et al.* Inhibition of telomerase limits the growth of human cancer cells. *Nature Med.* **5**, 1164–1170 (1999).
47. Kim, N. W. *et al.* Specific association of human telomerase activity with immortal cells and cancer. *Science* **266**, 2011–2015 (1994).
48. Yamashita, T. *et al.* RNA-dependent RNA polymerase activity of the soluble recombinant hepatitis C virus NS5B protein truncated at the C-terminal region. *J. Biol. Chem.* **273**, 15479–15486 (1998).
49. Azuma-Mukai, A. *et al.* Characterization of endogenous human Argonautes and their miRNA partners in RNA silencing. *Proc. Natl Acad. Sci. USA* **105**, 7964–7969 (2008).